DOI: 10.1021/ma900815g

Macromolecules
ARTICLE

Py-GC/MS and MALDI-TOF/TOF CID Study of Poly(phenyl sulfone) Fragmentation Reactions

Sparkle T. Ellison,[†] Anthony P. Gies,*[,‡] David M. Hercules,[‡] and Stephen L. Morgan[†]

[†]*Department of Chemistry and Biochemistry, University of South Carolina, Columbia, South Carolina 29208, and* [‡]*Department of Chemistry, Vanderbilt University, Nashville, Tennessee 37235*

Received April 14, 2009; Revised Manuscript Received May 20, 2009

ABSTRACT: We report a combination of the evaporation−grinding MALDI sample preparation method, MALDI-TOF/TOF CID, and Py-GC/MS to examine the fragmentation mechanisms of poly(phenyl sulfone) (PPSF). The fragmentation pattern for PPSF was compared to that of polysulfone from our previous study to test the generality of the established degradation mechanism. Py-GC/MS allowed prediction of preferred fragmentation of PPSF location based upon polysulfone fragmentation patterns and identification of four sulfide-containing fragments that were not seen in polysulfone. The identification of sulfide moieties in the Py-GC/MS of PPSF indicates that the lack of an isopropylidene group, like that found in polysulfone, may decrease the stability the sulfone group, thus resulting in its reduction to the more stable sulfide. Our study indicates that both poly(aryl ether sulfone)s preferentially cleave at the phenyl−sulfone bond, followed by the phenyl−oxygen bond. We were also able to make predictions on the CID fragmentation of low molecular weight linear PPSF using fragmentation patterns that were established by Py-GC/MS.

Introduction

Poly(aryl ether sulfone)s (PAES) are a unique family of thermoplastics that are distinguishable from most aromatic polymers by the presence of a para-linked diaryl sulfone in the backbone. Only three PAES, shown in Figure 1, are commercially available: polysulfone (PSF), poly(ether sulfone) (PES), and poly(phenyl sulfone) (PPSF). These polymers have three distinct performance characteristics that set them apart from other aromatic polymers: high glass transition temperatures, long-term thermal oxidative endurance, and high temperature melt thermal stability.[1] When these properties are desired for industrial applications, PSF is usually the first PAES considered due to its low cost and existing extensive use. If greater chemical resistance, flame retardation, or heat resistance is needed, PES is selected over PSF. PPSF offers superior chemical, impact and heat resistance, and overall ability to retain ductility than PSF and PES. However, because of its high production cost, PPSF is generally reserved for use in applications where both PSF and PES fail to meet requirements.[1−3]

The degradation pattern of a polymer is an important characteristic to consider when choosing a polymer for product manufacturing. Traditionally, analytical pyrolysis has been employed to study the degradation of high-temperature polymeric materials which are difficult to fragment and study by any other means. Previous analyses of the thermal degradation of PSF, PES, and their blends or modifications have been published.[4−11] These studies utilized pyrolysis−gas chromatography/mass spectrometry (Py-GC/MS), Py-GC with flame ionization (FID) and flame photometric detection (FPD), and thermal gravimetric analysis (TGA) to analyze degradation products. However, it has been shown that a combination of both Py-GC/MS and TOF/TOF CID is necessary to provide a better understanding of the degradation processes of polymers.[12−15]

*Corresponding author: Tel (615) 343-5980; e-mail A.Gies@Vanderbilt.edu.

In an earlier paper, we used Py-GC/MS and MALDI-TOF/TOF CID to develop fragmentation reaction mechanisms of PSF.[15] The literature is decidedly lacking on the subject of PPSF degradation and analysis. The focus of the present study is on the application of our multiple main-chain fragmentation models to interpret and compare the high kinetic energy degradation processes of Py-GC/MS with the low kinetic energy fragmentation of TOF/TOF CID of PPSF and to test the generality of our previous mechanisms for PAES.

Experimental Section

Poly(phenyl sulfone) Synthesis. Model poly(phenyl sulfone) (PPSF) samples were synthesized via step-growth polymerization.[16] All reagents were obtained from commercial sources. The experimental conditions (i.e., monomer reaction ratios) were chosen, based upon Carother's equation, to produce the desired degree of polymerization.[16] Number-averaged molecular weights (M_n) were determined by size exclusion chromatography (SEC) and MALDI-TOF MS.

Py-GC/MS Measurements. Poly(phenyl sulfone) samples were analyzed using a Pyroprobe 2000 heated filament pyrolyzer (CDS Analytical, Oxford, PA) interfaced to an HP G1800C GC/MSD instrument (Palo Alto, CA) (electron ionization 70 eV) via a CDS 1500 valve interface (CDS Analytical, Oxford, PA), kept at a constant temperature of 270 °C. The injection port and transfer line temperatures were both set at 270 °C. A 0.5 mg polymer sample and quartz wool (which prevents any nonvolatile components from escaping the sample tube) were placed into a quartz sample tube; the tube was positioned inside of the coil filament and allowed to purge under helium for 3 min in the pyrolysis interface. The pyrolyzer coil was then heated to 500 °C at a rate of 20 °C/ms and held for 10 s. The mass spectrometer was scanned from 40 to 500 Da. After obtaining the GC/MS, the quartz insert was removed from the pyrolyzer coil and flame-cleaned. Additional samples were analyzed with the pyrolyzer coil temperature raised in 100 °C increments, until a temperature of 1200 °C was reached. For the PPSF sample, additional measurements were made at final pyrolysis temperatures of

 Published on Web 06/09/2009

850 and 950 °C. The separation was performed using a 30 m (0.25 i.d. and 0.25 μm film thickness) HP-5 MS capillary column (Agilent, Palo Alto, CA). The column oven temperature was programmed to start at 50 °C for 3 min, ramp at 7.0 °C/min for 31.50 min, and held at 270 °C for 4.50 min, for a total heating cycle of 39 min.

MALDI-TOF/TOF CID Measurements. All samples were analyzed using an Applied Biosystems 4700 Proteomics Analyzer MALDI-TOF/TOF MS (Applied Biosystems, Framingham, MA) equipped with a 355 nm Nd:YAG laser. All spectra were obtained in the positive ion mode using an accelerating voltage of 8 kV for the first source and 15 kV for the second source and a laser intensity of ~10% greater than threshold. The grid voltage, guide wire voltage, and delay time were optimized for each spectrum to achieve the best signal-to-noise ratio. The collision energy in both TOF instruments is defined by the potential difference between the source acceleration voltage and the floating collision cell; in our experiments this voltage difference was set to 1 kV. Air was used as a collision gas at pressures of 1.5×10^{-6} and 5×10^{-6} Torr (which will later be referred to as "low" and "high" pressure, respectively). All spectra were acquired in the reflectron mode with a mass resolution greater than 3000 fwhm; isotopic resolution was observed throughout the entire mass range detected. External mass calibration was performed using protein standards from a Sequazyme Peptide Mass Standard Kit (Applied Biosystems) and a three-point calibration method using Angiotensin I (m = 1296.69 Da), ACTH (clip 1-17) (m = 2093.09 Da), and ACTH (clip 18-39) (m = 2465.20 Da). Internal mass calibration was subsequently performed using a PEG standard (M_n = 2000; Polymer Source, Inc.) to yield monoisotopic masses exhibiting a mass accuracy better than $\triangle m = \pm 0.05$ Da. The instrument was calibrated before every measurement to ensure constant experimental conditions. All samples were run in Dithranol (Aldrich) doped with sodium trifluoroacetate (NaTFA, Aldrich). The samples were prepared using the evaporation−grinding method (E−G method) in which a 2 mg sample of poly(phenyl sulfone) was ground to a fine powder using an agate mortar and pestle. Then molar ratios (with respect to the moles of polymer) of 25 parts matrix and 1 part cationizing agent (NaTFA) were added to the finely ground polymer along with 60 μL of distilled tetrahydrofuran (THF, Fisher). The mixture was ground until the THF evaporated, after which the residue that accumulated on the sides of the mortar was pushed down to the bottom of the

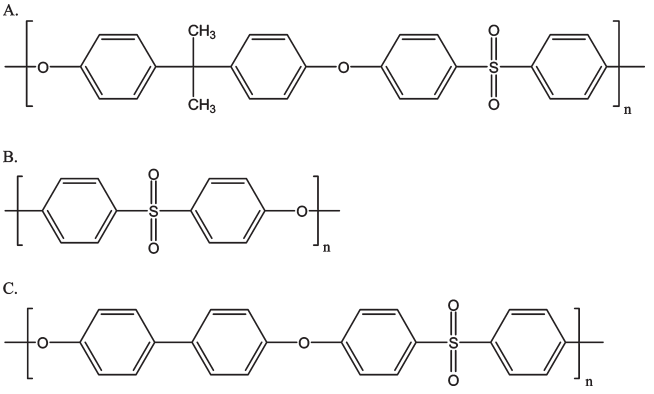

Figure 1. Structure of (A) polysulfone (PSF), (B) poly(ether sulfone) (PES), and (C) poly(phenyl sulfone) (PPSF).

Table 1. Structural Assignments for Pyrolysis Products Observed in the Py-GC/MS Pyrograms Reported in Figure 2

Species		Ret. Time (min)	Structure	M (Da) (* = no Na^+)	850 °C Peak Intensity (% Base Peak)	950 °C Peak Intensity (% Base Peak)
1-2	Sulfur Dioxide	1.37	SO_2	*64.0	85.0-major	80.4-major
1-3	Benzene	2.19		*78.1	26.1-small	39.1-medium
1-7	Toluene	3.37		*92.1	3.5-minor	5.3-minor
1-13	Styrene	5.80		*104.1	0.7-trace	1.5-trace
1-15	Benzenethiol	7.54	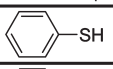	*110.0	1.0-trace	1.0-trace
1-1	Phenol	8.51	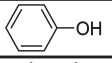	*94.1	100-major	100-major
1-8	Naphthalene	12.66	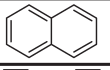	*128.2	0.75-trace	5-minor
1-5	Biphenyl	16.47		*154.2	21.2-small	26.6-small
1-4	diphenylether	16.95	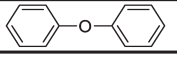	*170.2	41.6-medium	35.8-medium
1-6	Dibenzofuran	18.95	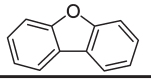	168.1	17.4-small	20.7-small
1-10	Diphenyl sulfide	20.14	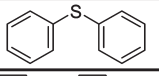	*186.1	3.2-minor	3.2-minor
1-11	*p*-hydroxyl diphenyl	22.20		*170.1	2.8-trace	3.1-minor
1-12	Dibenzothiophene	22.80	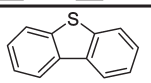	*184.0	1.4-trace	2.7-trace
1-14	Diphenyl disulfide	23.94	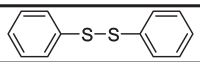	*218.0	1.8-trace	1.4-trace
1-9	*p*-diphenyl phenylether	28.90	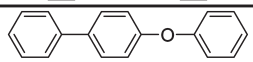	*246.1	7.9-small	3.8-minor

vessel. The mixture was then ground again to ensure homogeneity. A sample of the mixture was then pressed into a sample well by spatula on the MALDI sample plate. MS and MS/MS data were processed using the Data Explorer 4.9 software (Applied Biosystems).

Results and Discussion

While previous Py-GC/MS studies have reported mechanistic information for the thermal degradation of PSF and PES,[6−8] to date none have studied the thermal degradation of PPSF. For our study, we will compare data from the unimolecular fragmentation of MS/MS to the multimolecular free radical reactions of Py-GC/MS. Py-GC/MS data will be presented first, followed by the results from MS/MS analysis that include fragmentation mechanisms and order of preferential bond cleavage. A comparison of these mechanisms with those of PSF[15] will also be included.

Pyrolysis-GC/MS. The pyrolysis products were identified using library matching software, where a match of 85% or greater was accepted. The following terminology will be used when relating the pyrolysis products shown in Table 1 with their peak intensities observed for the PPSF pyrograms shown in Figure 2: *major* (>50% base peak, BP); *medium* (30−50% BP); *small* (7−30% BP); *minor* (3−7% BP); and *trace* (<3% BP). We will first discuss the major observed pyrolysis product peaks and then discuss the unexpected trace pyrolysis products produced from the thermal degradation of PPSF.

Pyrolysis is a higher energy bond fragmentation method than MS/MS. As set pyrolysis temperatures increase, more kinetic energy is available to cleave bonds. As such, multiple bond-breaking reactions dominate Py-GC/MS. When developing fragmentation mechanisms from polymer pyrolysis, two factors are important: (1) bond dissociation energies (the weakest bonds generally break first) and (2) stability of the generated radicals.[17] Using previously determined thermal degradation mechanisms for the structurally similar PSF,[15] one can predict the order of bond breaking (weakest to strongest) for PPSF. Like PSF, the expected order of bond breaking for PPSF to be as follows: Ph−SO_2, Ph−O, and Ph−Ph.

Thermal degradation of PPSF requires temperatures in excess of 650 °C. This is higher than that seen with PSF, owing to the fact that PPSF is a much more thermally stable polymer. Appreciable amounts of characteristic pyrolysis products are not obtained at temperatures below 800 °C. Parts A and B of Figure 2 display programs of PPSF taken at 850 and 950 °C, respectively, to show the pyrolysis composition at ideal pyrolysis temperatures. At higher set pyrolysis temperatures (above 1000 °C), excessive fragmentation occurs, thus limiting obtainable information about the polymer in the pyrogram. Scheme 1 shows the first step in the thermal decomposition of PPSF: the breaking of the Ph−SO_2 bond. MALDI-TOF/TOF CID has a much lower kinetic energy than Py-GC/MS; thus, PPSF would initially break via Scheme 1A. Depending on the nature of the end groups, this could result in the production of 3-1 (as shown in Table 3). However, under the high kinetic energy conditions of pyrolysis, at 700−950 °C, there will be multiple main-chain fractures, and the initial fragments produced will be species 1-2 (SO_2) and 3-6, as shown in Scheme 1B. Species 1-2 is the most intense pyrolysis product from 650 to 700 °C and then begins to decrease in intensity at 750 °C. Species 1-2 is still a major pyrolysis product, regardless of decomposition temperature. Unlike MALDI-TOF/TOF CID, the "pulse" of kinetic energy for Py-GC/MS has a much longer duration,

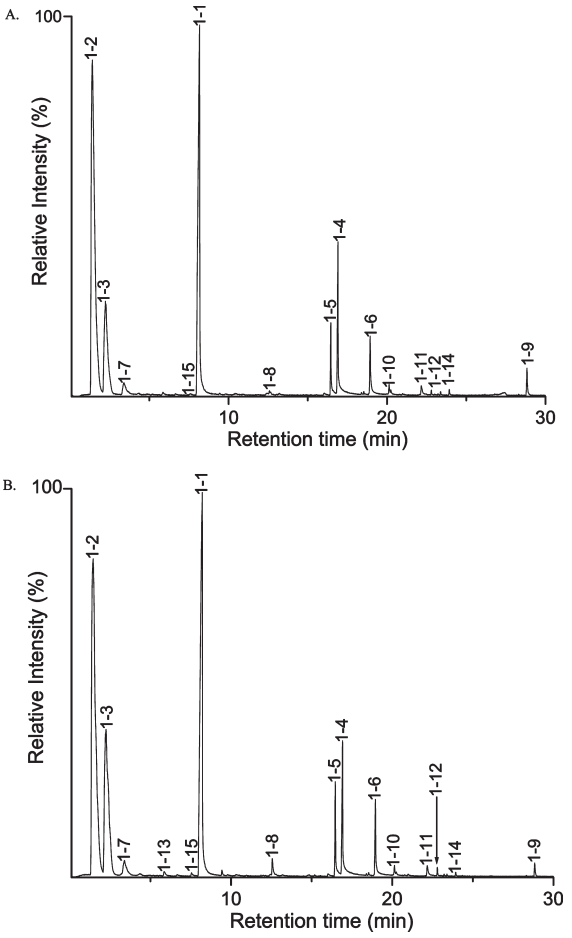

Figure 2. Py-GC/MS pyrograms of PPSF taken at (A) 850 and (B) 950 °C. Sample size: 0.5 mg.

thus allowing time for species 3-6 to undergo further degradation reactions.

Scheme 2 shows the secondary mechanism in PPSF thermal decomposition: competition for main-chain scission at the Ph−O (Scheme 2A) vs Ph−Ph (Scheme 2B) bond. A single cleavage of the Ph−O bond in species 3-6 will produce species 1-1 and 1-9 (Scheme 2Ai). The peak intensity for species 1-9 decreases from 7.9% to 3.8% as the temperature increases. The decrease in peak intensity implies that 1-9 further degrades at higher kinetic energies (vide infra). When species 3-6 undergoes multiple main-chain scissions of the Ph−O bond (Scheme 2Aii), fragment species 1-1, 1-3, 1-5, and 1-11 are produced. The intensities for peaks 1-3, 1-5, and 1-11 increase at higher temperatures, which is consistent with a fragmentation mechanism consistent with production from a secondary (higher energy) reaction. Species 1-3 peak intensity increases from 26.1% to 39.1%. Species 1-5 and 1-11 increase to a much lesser extent than 1-3. This slight increase suggests that these two species can undergo further degradation at higher kinetic energies. Contributions from further degradations of 1-5, 1-9, and 1-11 via tertiary reactions can also increase the relative peak intensity of 1-3. The multiple pathways, both secondary and tertiary reactions, to produce species 1-1 contribute to its high peak intensity at temperatures above 750 °C. There is also a competing secondary mechanism: scission at the Ph−Ph bond (Scheme 2B). Cleavage at the Ph−Ph would produce species 1-4. Because species 1-4 is the product of a secondary fragmentation reaction, the peak intensity should increase as pyrolysis temperature (kinetic energy) increase. As shown

Scheme 1. Major Pyrolysis Fragmentation Mechanisms of Poly(phenyl sulfone): (A) Low-Energy Cleavage of a Single Ph−SO_2 Bond and (B) High-Energy Cleavage of Multiple Ph−SO_2 Main-Chain Bonds for Production of Species 1-2 and 3-1 (in Figure 2A,B)

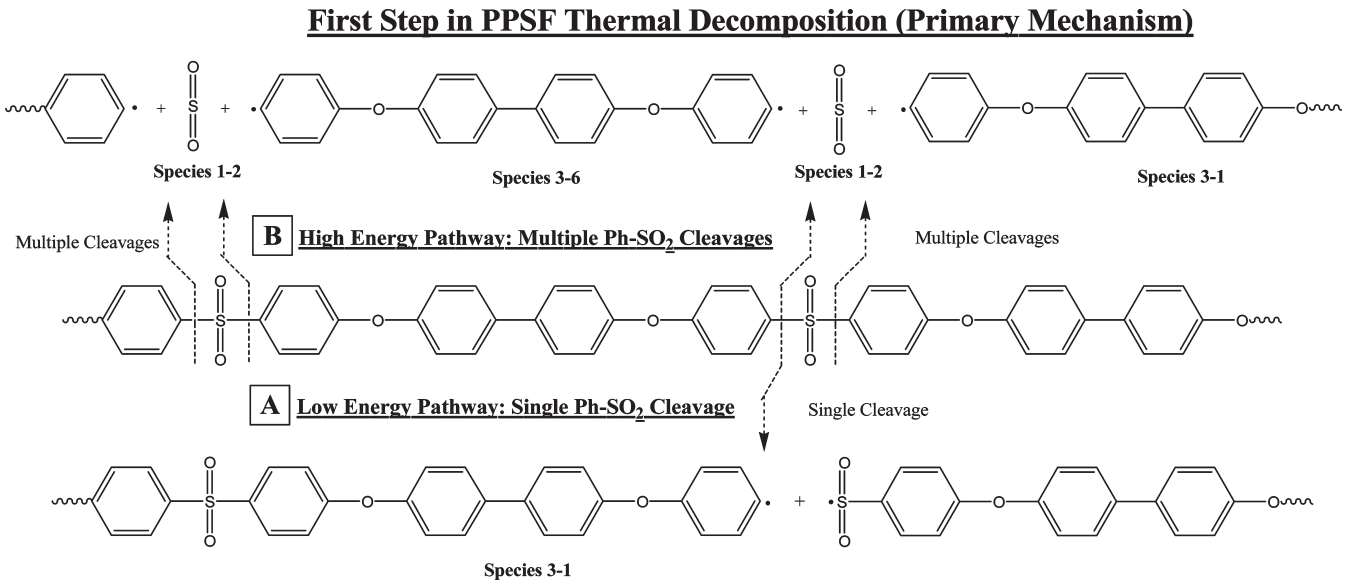

Scheme 2. Secondary (High-Energy) Pyrolysis Fragmentation Mechanisms of Poly(phenyl sulfone): (A) Species 3-6 Can Undergo (i) a Single Cleavage at the Ph−O Bond To Produce Species 1-1 and 1-9 or Undergo (ii) Multiple Cleavages of the Ph−O Bond To Produce Species 1-1, 1-3, 1-5, and 1-11; (B) Cleavage of the Ph−Ph Bond To Produce Species 1-4[a]

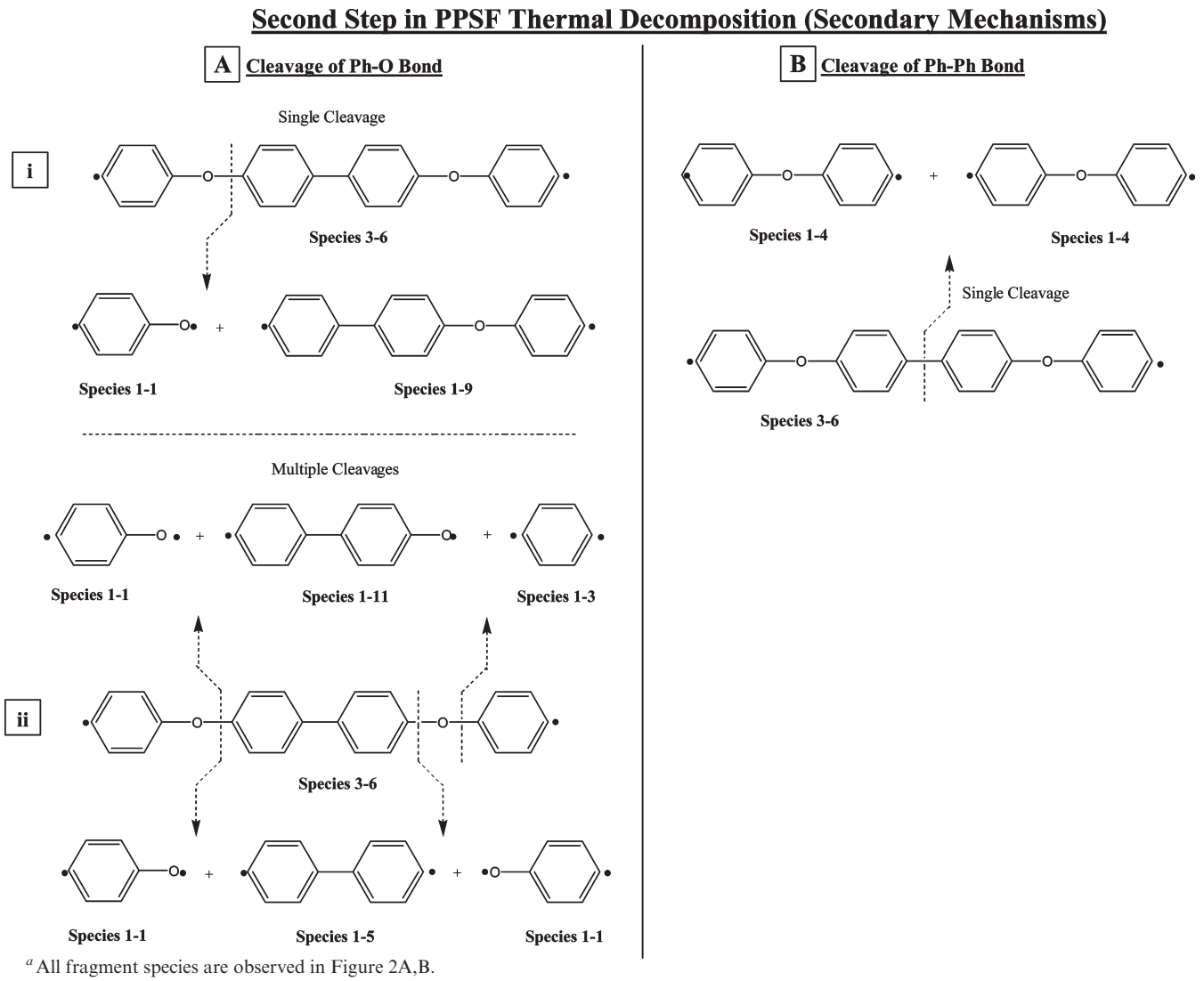

[a] All fragment species are observed in Figure 2A,B.

in Table 1, the intensity of species 1-4 decreases as the pyrolysis temperature increases from 850 to 950 °C. This decrease in peak intensity is attributed to further degradation of species 1-4. Scheme 3B displays the degradation of species 1-4, by cleavage of the Ph−O bond, to produce species 1-1 and 1-3.

At 950 °C and above, there is sufficient energy for fragment species 1-4, 1-5, 1-9, and 1-11 to undergo additional degradation as shown in Scheme 3. Scheme 3A shows that species 1-9 can undergo cleavage at both the Ph−O and Ph−Ph bonds. Cleavage at the Ph−Ph bond (Scheme 3Ai) produces species 1-3 and 1-4. Cleavage of the Ph−O bond (Scheme 3Aii) can produce species 1-1, 1-3, 1-5, and 1-11.

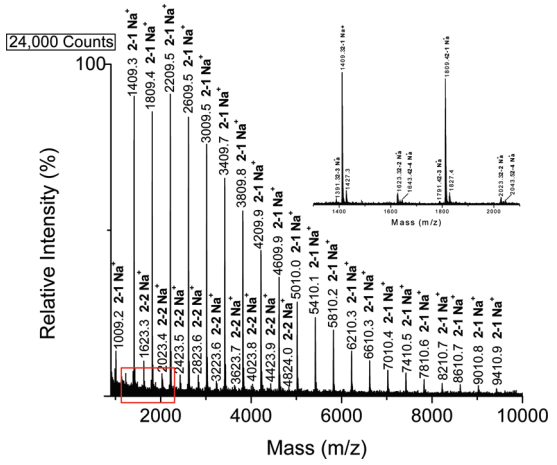

Figure 3. MALDI-TOF mass spectrum for PPSF.

Species 1-4 and 1-11, produced from both the secondary fragmentations and the tertiary fragmentations, can then undergo subsequent fragmentation, as shown in Scheme 3B and 3Ci, respectively. Scheme 3B shows that species 1-4 will cleave at a Ph−O bond to form species 1-1 and 1-3. Scheme 3Ci shows that once 1-11 is produced, the Ph−Ph bond can be cleaved to produce species 1-1 and 1-3. As mentioned above, species 1-9 can also experience a single cleavage at the Ph−O bond to produce species 1-5 (Scheme 3Aii). Species 1-5 can further degrade into species 1-3 by cleavage of the Ph−Ph bond (Scheme 3Cii). The multiple pathways to produce 1-3 contribute to its increase in intensity that is seen between 850 and 950 °C.

At higher pyrolysis temperatures, an increase in cyclization and recombination reactions can take place. For instance, the peak intensity for species 1-6 increases from 17.4% to 20.7%. Species 1-6 is formed by the cyclization of the diradical of species 1-4 (diphenyl ether). Naphthalene, species 1-8, is the product of recombination of species 1-3. As a result, as temperatures increase, the peak intensity for 1-8 increases from trace levels (0.75%) to minor levels (5%).

A few unexpected species at the trace level were identified using Py-GC/MS. Previously unreported sulfonated species were identified in the Py-GC/MS of PSF.[15] For PPSF, these species were not seen; however, four sulfide-containing species, species 1-10, 1-12, 1-14, and 1-15, were identified. At all temperatures, the peak intensities for these four species were below 4% of the base peak. Previously, studies on PES have identified sulfide degradation products, produced via reduction of the sulfone group by hydrogen atoms.[7,8,18] Because of the similarity between PES and PPSF, these same

Scheme 3. Tertiary (High-Energy) Pyrolysis Fragmentation Mechanisms of Poly(phenyl sulfone): (A) Species 1-9 Can Undergo a Single Main-Chain Fragment of the (i) Ph−Ph Bond To Produce Species 1-3 and 1-4 or the (ii) Ph−O Bonds To Yield Fragment Species 1-3 and 1-11 or Species 1-1 and 1-5; (B) Species 1-4 Undergoes Cleavage at Only the Ph−O Bond To Produce Species 1-1 and 1-3; and (C) Species 1-11 Can Undergo a Single Main-Chain Fragment of the (i) Ph−Ph bond, as Well, To Produce Species 1-1 and 1-3[a]

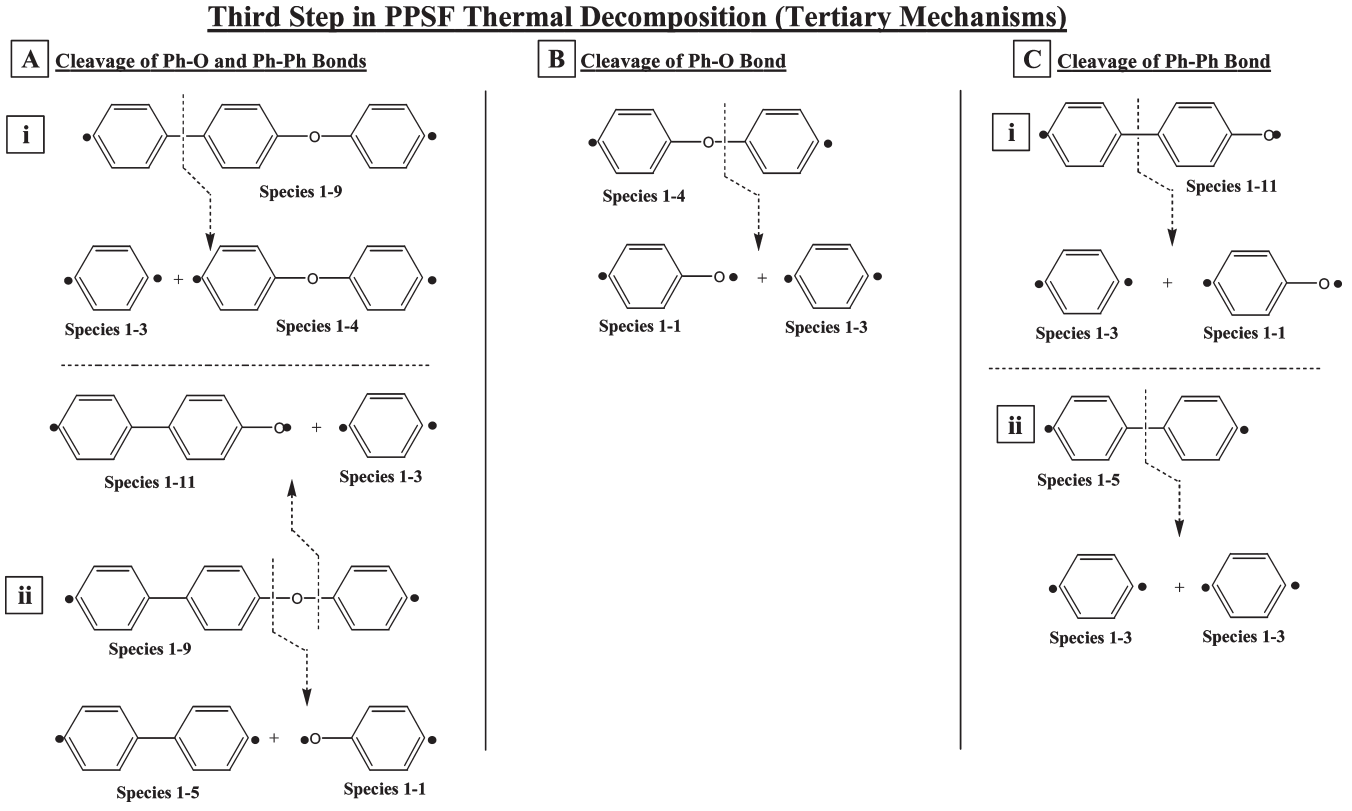

[a] Species 1-5 can undergo a single main-chain fragment of the (ii) Ph−Ph bond to produce species 1-3.Tertiary fragment species show greater peak intensities in Figure 2B than in Figure 2A.

Table 2. Structural Assignments for Peaks in the MALDI-TOF Mass Spectrum Reported in Figure 3

Species	Structure (M)	$(M+Na)^+$ (Da)
2-1	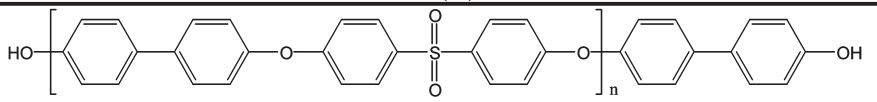	**609.1** (n = 1) **1009.2** (n = 2) **1409.3** (n = 3) **1809.4** (n = 4) ... **9810.9** (n = 24)
2-2	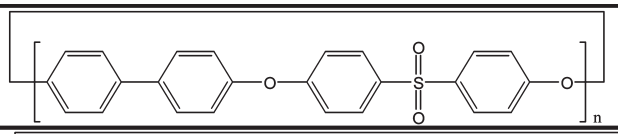	**423.1** (n = 1) **823.2** (n = 2) **1223.2** (n = 3) **1623.3** (n = 4) ... **9624.9** (n = 24)
2-3	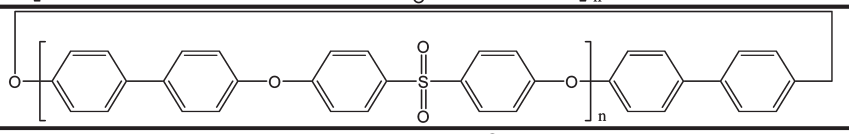	**591.1** (n = 1) **991.2** (n = 2) **1391.3** (n = 3) **1791.4** (n = 4) ... **9793.0** (n = 24)
2-4	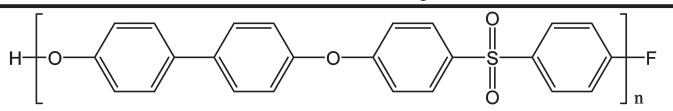	**443.1** (n = 1) **843.2** (n = 2) **1243.3** (n = 3) **1643.4** (n = 4) ... **4844.0** (n = 12)

Table 3. Structural Assignments for Peaks in the MALDI-TOF/TOF Mass Spectrum Reported in Figure 4

Species	Structure (M)	Na^+ (* = carbocation with no Na^+) M (Da)
3-1	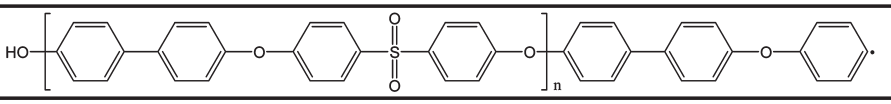	**684.2** (n = 1) **1084.2** (n = 2) **1484.3** (n = 3)
3-2	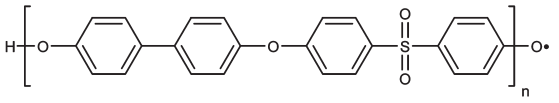	**440.1** (n = 1) **840.2** (n = 2) **1240.2** (n = 3)
3-3	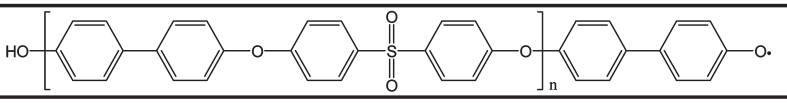	**608.1** (n = 1) **1008.2** (n = 2) **1408.3** (n = 3) **1808.4** (n = 4)
3-4	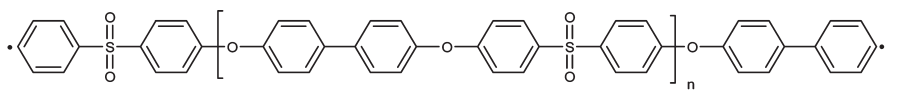	* **784.2** (n = 1) **807.2** (n = 1) ***1184.2** (n = 2) **1207.2** (n = 2)
3-5	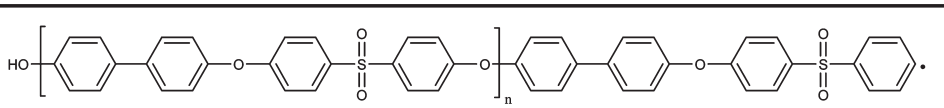	**824.2** (n = 1) **1224.2** (n = 2) **1624.3** (n = 3)
3-6	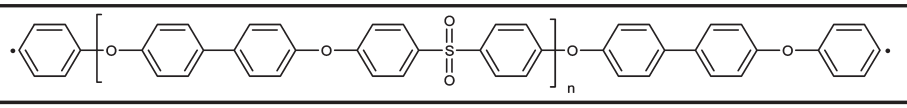	**759.2** (n = 1) **1159.3** (n = 2) **1559.4** (n = 3)
3-7	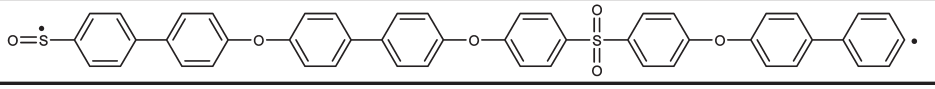	**316.1** (n = 1) **716.2** (n = 2) **1116.3** (n = 3)

degradation mechanisms are expected to apply to PPSF as well. The presence of the isopropylidene group may stabilize PSF during degradation at higher temperatures; however, for PES and PPSF, the reduction of the sulfone group to the more stable sulfide moiety is necessary to achieve the same stability seen in PSF.

MALDI-TOF/TOF CID. MALDI-TOF mass spectrometry yields a wealth of information on the mass, structure, and end groups of large molecules generated in chemical reactions, and this information can provide a wealth of knowledge needed to cultivate a fragmentation pattern. Figure 3 displays a representative spectrum of PPSF, including an enlarged section to highlight the smaller peaks that are dwarfed in the full-scale spectrum. Table 2 contains the identities of the label peaks. For CID fragmentation, MALDI-TOF MS can be used to determine the "ideal" peak series for fragmentation.

CID fragmentation was conducted on a variety of poly (phenyl sulfone) precursor ions; however, it was discovered that the lower effective kinetic energy of our TOF/TOF CID

instrument (with respect to PPSF fragmentation) was limited to the lower molecular weight portion of the PPSF molecular mass distribution. Molecular masses above 2000 Da did not generate usable CID spectra for PPSF. Table 3 summarizes the masses of the ion peak series observed in MALDI-TOF/TOF CID mass spectra from a linear poly(phenyl sulfone) oligomer ion: PPSF, 1409.3 Da ($n = 3$). All values listed are for sodium-cationized poly(phenyl sulfone) ions, unless noted otherwise.

MS/MS facilitates the study of unimolecular polymer degradation (due to gas phase/low pressure dilution) in which a complete array of fragment ion masses is detected in one single, highly resolved spectrum.[13] On the basis of the Py-GC/MS results (Schemes 1−3), one would expect primary CID fragmentation of PPSF to occur at the Ph−SO_2 bond. The CID "pulse" input of kinetic energy is much shorter in duration than that experienced in Py-GC/MS; therefore, fragmentation at the Ph−O and Ph−Ph linkages will occur at a much lower rate in CID. Most of the secondary reactions should involve radicals formed by the cleavage of the Ph−SO_2 bond.

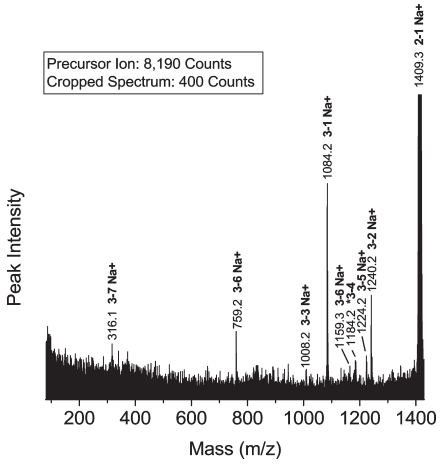

Figure 4. MALDI-TOF/TOF mass spectrum for linear PPSF (1409.3 Da precursor ion) at a collision gas pressure of 5×10^{-6} Torr.

The MS/MS spectrum of linear PPSF (Figure 4) shows the most intense product peak at 1084.2 Da corresponding to fragment 3−1 ($n = 2$), which is formed by a single main-chain fragment at the Ph−SO_2 bond. This fragment is comparative to the fragment that resulted in the two most intense peaks observed in the MS/MS of linear PSF in our previous study.[15] Similarly, the CID spectrum of the linear PPSF precursor ion, with the next higher repeat unit at 1809.4 Da ($n = 4$) (Figure S5 in the Supporting Information), shows the most intense product peak at 1484.3 Da, which corresponds to 3−1 ($n = 3$). The intensity of the 3−1 fragment peak series confirms that this was the major fragmentation pathway. The third most intense peak is at 759.2 Da, which corresponds to fragment 3−6 ($n = 1$). Fragment 3−6 is the result of the cleavage of two Ph−SO_2 bonds, to form a radical on each phenyl terminal group. Note that cleavage of the Ph−SO_2 bond in PPSF resulted in $Ph^{\bullet}$ as opposed to a SO_2 radical. Linear PSF had two fragments with $SO_2^{\bullet}$ on the end, one of which was a diradical.[15] The lack of a $SO_2^{\bullet}$ end may be attributed to its instability, as proposed by the Py-GC/MS data. In pyrolysis, the extended "pulse" of kinetic energy is much longer, allowing for the reduction of the sulfone group through

Scheme 4. TOF/TOF CID Fragmentation for Linear PPSF Oligomer

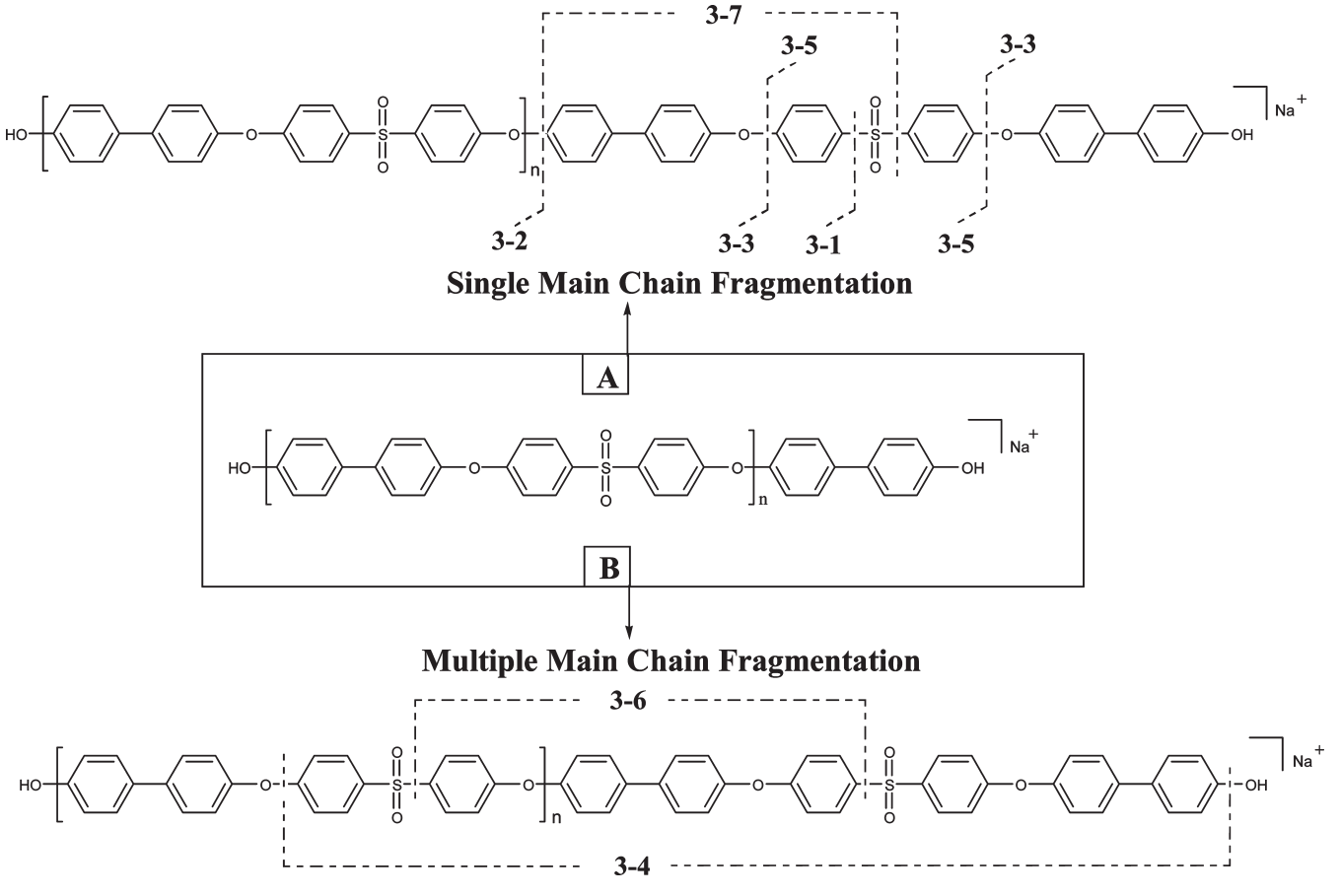

interaction with hydrogen atoms. Not only is MS/MS a unimolecular process, there is not as much time allowed for the interaction of this end group with other species, thus resulting in the loss of SO_2.

Of the seven fragment series noted in Table 3, three series, 3-2, 3-3, and 3-5, are formed by a single main-chain fragmentation at the Ph−O cleavage, whereas series 3-4 is formed by two main chain cleavages at the Ph−O bond and series 3-7 is formed by a main chain cleavage at the Ph−O bond and cleavage at the Ph−SO_2 followed by loss of an oxygen. The presence of the diphenyl linkage weakens the adjacent Ph−O bond, thus making it easier to break. Series 3-7 is the only fragment to have a sulfur-containing radical. The preferentially cleavage of this bond but absence of $SO_2^{\bullet}$ fragments supports the pyrolysis results which point to the reduction of SO_2 to sulfides. Fragments resulting from the Ph−Ph cleavage were not identified. The fragmentation of the Ph−O bonds show that MS/MS has enough energy to induce cleavage at these higher strength bonds; however, the predominance of Ph−SO_2 bond fragmentation shows that this bond prefers to break. The fragmentation pattern for linear PPSF is shown in Scheme 4.

Conclusions

The multimolecular free radical reactions in pyrolysis were compared with the unimolecular fragmentation reactions of MS/MS to establish fragmentation patterns for PPSF. Comparisons were made with the fragmentation of PSF, a structurally similar polymer, to establish the generality of the proposed fragmentation pattern. Using Py-GC/MS, we were able to not only predict preferred fragmentation located based PSF fragmentation patterns, but we also identified four sulfide-containing fragments that were not seen in PSF. We found that CID fragmentation of higher molecular weight PPSF is not easy due the high energy needed to fragment the bonds of this high strength polymer. Further, we were also able to make predictions on the CID fragmentation of low molecular weight linear PPSF using fragmentation patterns that were establish by Py-GC/MS.

Acknowledgment. The authors thank Stephen M. June and Timothy E. Long, at Virginia Polytechnic State University, for donation of the PPSF samples.

Supporting Information Available: Details of the poly (phenyl sulfone) overall MALDI-TOF mass spectra, uncropped TOF/TOF CID spectra, and Py-GC/MS electron ionization fragmentation spectra. This material is available free of charge via the Internet at http://pubs.acs.org.

References and Notes

(1) El-hibri, M. J.; Nazabal, J.; Equiazabal, J. I.; Arzak, A. Poly (aryl ether sulfone)s. In *Handbook of Thermoplastics*; Olabisi, O., Ed.; Marcel Dekker: New York, 1997; pp 893−950.
(2) Clendinning, R. A.; Dickinson, B. L. Poly (aryl ether sulfone)s. In *Polymeric Materials Encyclopedia*; Salamone, J. C., Ed.; CRC Press: Boca Raton, FL, 1996; pp 5562−5569.
(3) Hishaw, R. J. An evaluation of polyphenylsulfone; US Department of Energy, BDX-613-2145 , **1979**.
(4) Lisa, G.; Avram, E.; Paduraru, G.; Irimia, M.; Hurduc, N.; Aelenei, N. *Polym. Degrad. Stab*. **2003**, *82*, 73–79.
(5) Botvay, A.; Máthé, A.; Pöppl, L.; Rohonczy, J.; Kubatovicx, F. *J. Appl. Polym. Sci*. **1999**, *74*, 1–13.
(6) Almén, P.; Ericsson, I. *Polym. Degrad. Stab*. **1995**, *50*, 223–228.
(7) Perng, L. H. *J. Appl. Polym. Sci*. **2001**, *81*, 2387–2398.
(8) Perng, L. H. *J. Polym. Sci., Part A: Polym. Chem*. **2000**, *38*, 583–593.
(9) Ohtani, H.; Ishida, Y.; Ushiba, M.; Tsuge, S. *J. Anal. Appl. Pyrolysis* **2001**, *61*, 35–44.
(10) Montaudo, G.; Puglisi, C.; Samperi, F. *Macromol. Chem. Phys*. **1994**, *195*, 1241–1256.
(11) Montaudo, G.; Puglisi, C.; Rapisardi, R.; Samperi, F. *Macromol. Chem. Phys*. **1994**, *195*, 1225–1239.
(12) Gies, A. P.; Vergne, M. J.; Orndorff, R. L.; Hercules, D. M. *Anal. Bioanal. Chem*. **2008**, *392*, 609–626.
(13) Gies, A. P.; Vergne, M. J.; Orndorff, R. L.; Hercules, D. M. *Macromolecules* **2007**, *40*, 7493–7504.
(14) Gies, A. P.; Ellison, S. T.; Vergne, M. J.; Orndorff, R. L.; Hercules, D. M. *Anal. Bioanal. Chem*. **2008**, *392*, 627–642.
(15) Ellison, S. T.; Gies, A. P.; Hercules, D. M.; Morgan, S. L. *Macromolecules* **2009**, *42*, 3005–3013.
(16) Yang, H. H. *Aromatic High-Strength Fibers*; John Wiley & Sons: New York, 1989; p 873.
(17) Wampler, T. P. *Applied Pyrolysis Handbook*, 2nd ed.; CRC Press: New York, 2007; pp 1−46.
(18) Blazevska-Gilev, J.; Bastl, Z.; Šubrt, J.; Stopka, P.; Pola, J. *Polym. Degrad. Stab*. **2009**, *94*, 196–200.